Moroccan Journal of Chemistry
ISSN : 2351-812X

Mor. J. Chem., 2023, Volume 11, Issue 01, Page 20-33
https://revues.imist.ma/index.php/morjchem

New compounds based on 1H-pyrrolo[2,3-b] pyridine as potent TNIK inhibitors against colorectal cancer cells. Molecular modeling studies

Reda El-Mernissi [1,*], Khalil El Khatabi [1], Ayoub Khaldan[1], Soukaina Bouamrane [1], Mohammed Aziz Ajana[1,*], Tahar Lakhlifi [1], Mohammed Bouachrine [1,2]

[1] University of Moulay Ismail, Faculty of Science, MCNSL, Meknes, Morocco
[2] EST Khenifra, Sultan Moulay Sliman University, Benimellal, Morocco
**Corresponding author, Email address: a.ajanamohammed@fs.umi.ac.ma*
***Corresponding author, Email address: re.elmernissi@edu.umi.ac.ma*

Received *26 Oct 2022,*
Revised *19 Dec 2022,*
Accepted *23 Dec 2022*

Citation*: El-Mernissi R., El Khatabi K., Khaldan A., Bouamrane S., Ajana M.A., Tahar Lakhlifi T., Bouachrine M., (2023) New compounds based on 1H-pyrrolo[2,3-b] pyridine as potent TNIK inhibitors against colorectal cancer cells. Molecular modeling studies, Mor. J. Chem., 14(1), 20-33. Doi: https://doi.org/10.48317/IMIST.PRSM/morjchem-v11i1.35380*

Abstract: Cancer is a disease caused by the incorrect transformation of cells that proliferate abnormally, and it is one of the leading causes of mortality worldwide. As a result, new compounds with potential anticancer activity must be designed. In this article, three – dimensional Quantitative Structure-Activity Relationship is used to study thirty-one compounds of 1H-pyrrolo[2,3-b]pyridine derivatives as potent TNIK inhibitors against colorectal cancer cells. Their pIC50 varied from 7.37 to 9.92. The two contours, Molecular Field Analysis (CoMFA) and Comparative Molecular Similarity Indices (CoMSIA) are critical in determining the nature of the groups that enhance or reduce activity. The models CoMFA and CoMSIA indicate strong reliability with ($Q^2 = 0.65$; $R^2 = 0.86$; $r_{test}^2 = 0.97$) and ($Q^2 = 0.74$; $R^2 = 0.96$; $r_{test}^2 = 0.95$), respectively. Based on the good findings produced by the contour maps generated by the approach model, we have suggested five drugs with strong activity against colorectal cancer cells. In addition, the ADMET characteristics of these newly designed compounds were examined in silico. These compounds were further evaluated by molecular docking, showing that two molecules, Y4 and Y5, exhibit favorable interactions with the targeted receptor and a high total score. Our vision is to develop new medicines with strong TNIK inhibitory activities that target Traf2 and Nck-interacting kinase TNIK as a therapeutic target.

Keywords: Cancer; 1H-pyrrolo[2,3-b]pyridine; 3D-QSAR; ADMET; Molecular docking

1. Introduction

The diagnosis of cancer reveals colorectal cancer (CRC) is one of the most frequent cancers worldwide, it affects men and women in different proportions (Jemal *et al.,* 2011), colon cancer is a significant issue in human health, with over 700,000 fatalities each year (Katanoda *et al.,* 2012), the majority of individuals with colorectal cancer who have distant organ metastases, or no lymph nodes may be treated with surgical resection used (Okuno, 2007), the percentage of patients with stage IV colorectal cancer have a 5-year survival rate of less than 15 percent (Koutras *et al.,* 2011; Omura, 2008). Colorectal cancer may be prevented by exercising regularly and eating a diet rich in fruits and vegetables, whereas cigarettes, alcohol, processed meat, and red meat consumption increase the chance of getting the disease.

Traf2 and Nck-interacting kinase (TNIK) have been found to be required for the development of colon cancer cell lines, and its inhibition, inhibits cancer cell proliferation and growth, colorectal cancers are caused by mutations in one of two signaling pathway: b-catenin (CTNNB1) and adenomatous polyposis coli (APC) genes(Morin *et al.,* 1997; Polakis, 2000). The colorectal cancer cells retain their reliance on Wnt (Dow *et al.,* 2015; de Lau, Peng, Gros, & Clevers, 2014; Wielenga *et al., 1999; Yamamoto et al., 2003)* signaling, although the loss of the adenomate coli polypose is the most precocious genetic event in colorectal cancer (Powell *et al.,* 1992). The study of oncogenic retroviruses had an impact on the discovery of Wnt signaling pathways, colorectal carcinogenesis is fueled in part by Wnt signaling, TNIK is the main regulator of Wnt signaling, and colorectal cancer cells rely on it for growth and proliferation (Kahn, 2014).

In recent years, several pharmaceutical companies have used TNIK inhibitors with different chemical structures against colorectal cancer cells for example PF-794 (Pfizer) and Celon Pharma (Bujak *et al.,* 2015). TNIK is being studied as a possible colorectal cancer treatment target (Masuda *et al., 2016)*. Recently various compounds based on pyrrole and pyridine displayed attractive efficacy both in vitro and in vivo and had the potential to treat breast cancer (Li *et al.,* 2023; Imai *et al.,* 2023;). The objective of this study is to predict compounds that are effective TNIK inhibitors against colorectal cancer cells. In the context of our ongoing interest in the development of anticancer drugs (EL-Mernissi *et al.,* 2021; El-Mernissi e*t al., 2021, 2022)*, a series of thirty-one 1H-pyrrolo [2,3-b] pyridine compounds were employed in the quest for medicines against colorectal cancer based on TNIK receptor inhibition (Yang *et al.,* 2021). To identify the binding mechanisms of compounds with the Traf2 and Nck-interacting kinase (TNIK) (PDB code: 2X7F), molecular docking was conducted by utilizing surflex-docking, and the reliability of the suggested compounds was obtained.

2. Experimental Methods

2.1 Materials

A series of 31 substituted 1H-pyrrolo [2,3-b] pyridine derivatives from the literature were tested to 3D-QSAR modeling. The database was split into two groups, with 26 chemicals chosen as a training set and the remaining 5 as a test set (Khaldan *et al.,* 2021; Khalil EL Khatabi *et al.,* 2021). The 3D-QSAR (CoMFA and CoMSIA) model was built using the training set. Furthermore, the test set is used to assess the model's prediction ability. The IC50 value was first measured in units (nM) and then converted to pIC50 (pIC50 = Log 1/IC50) (M). The molecular structure of the agent for the study is shown in **Figure 1**, and **Table 1** lists the various structures for the test and training compounds, as well as their biological activity (pIC50)(M).

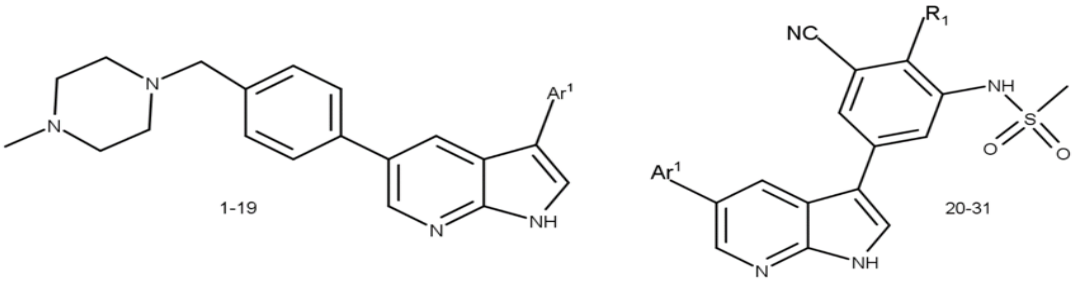

Figure 1. Structure of the studied compounds.

Table 1. The structure and activities of studied compounds.

N°	Ar^1	pIC50(M)	N°	Ar^1	R_1	pIC50(M)
1*	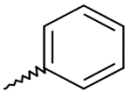	7.85	16	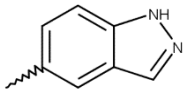	-	9.36
2	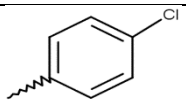	7.85	17	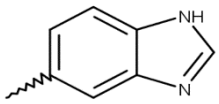	-	8.42
3	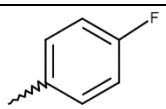	7.72	18	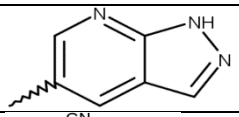	-	8.10
4	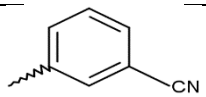	9.04	19	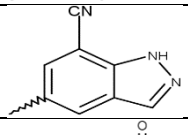	-	9.64
5	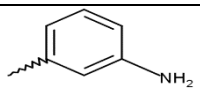	7.82	20	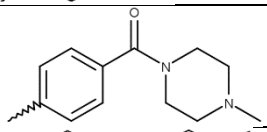	H	9.68
6	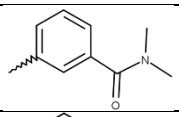	7.37	21	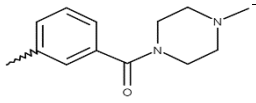	H	9.60
7	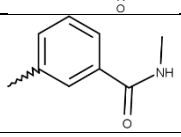	7.57	22	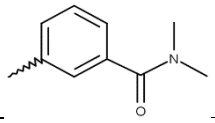	H	9.74
8	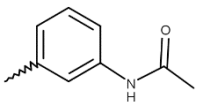	7.92	23	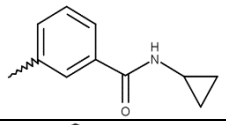	H	9.92
9	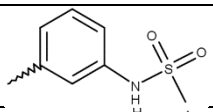	8.15	24	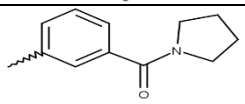	H	9.68
10*	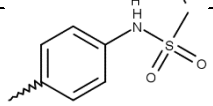	7.74	25	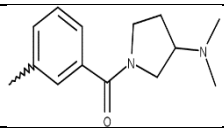	H	9.66
11*	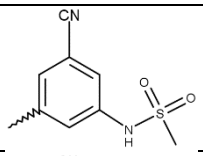	9.89	26	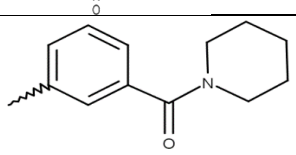	H	9.66
12*	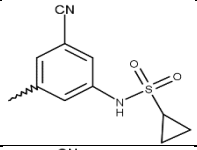	9.72	27	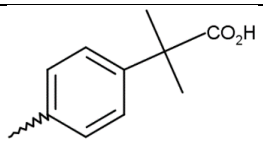	H	9.33
13*	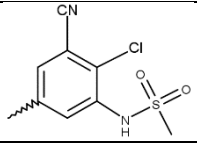	9.37	28	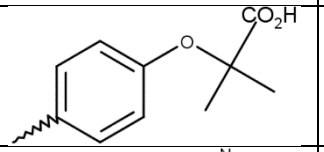	H	9.48
14	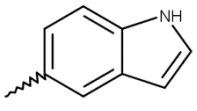	8.28	29*	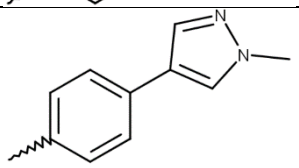	Cl	9.10

15	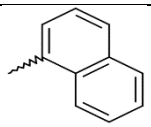	7.51	30	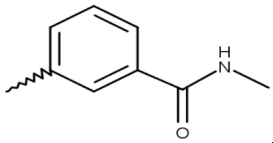	Cl	9.52
			31	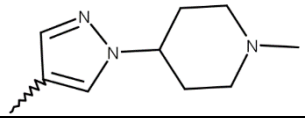	Cl	9.17

2.2 Minimization and alignment

Using the Gasteiger-Huckel partial atomic charges (Purcell & Singer, 1967) in the Sybyl (Cronin et al., 2018) software, all molecular structures are minimised under the conventional Tripos force field(Clark, Cramer, & Van Opdenbosch, 1989). Molecular alignment is one of the most important factors in 3D-QSAR studies (El Khatabi et al., 2020; EL-Mernissi et al., 2020; K El Khatabi et al., 2021). To align the database, the most active molecule 23 was utilised. **Figure 2** depicts the core and alignment of all compounds.

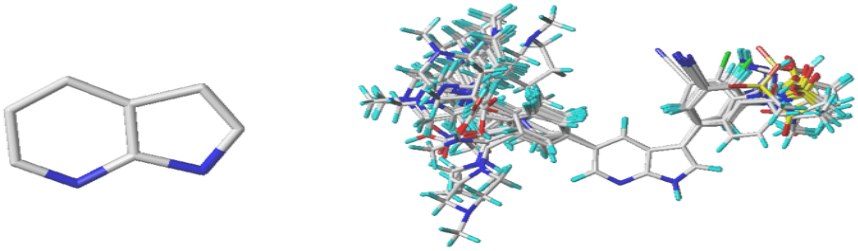

Figure 2. Core and the alignment of molecules

2.3 3D QSAR study

The CoMFA(Cramer, Patterson, & Bunce, 1988; Khaldan & Lakhlifi, 2020) and CoMSIA analysis is used to create 3D QSAR models(Bouamrane et al., 2022, Klebe, Abraham, & Mietzner, 1994), to predict new compounds, and to explore various fields, such as steric and electrostatic for the CoMFA model, while CoMSIA gives steric, electrostatic, hydrophobic, H–bond donors and acceptors. To achieve a linear correlation between the dependent variable (pIC50) and the independent variables (contours), the partial least squares analysis (PLS)(Bush & Nachbar, 1993) regression method was used. The process of non-cross-validation was given to evaluate the coefficient of determination (R^2), the value F (Fischer test and lowest value of the standard error of estimates (SEE), while to determine the cross-validated correlation coefficient (Q^2) and the optimum number of components N, a cross-validation method was used. Furthermore, a test set was used for external validation to calculate r^2_{ext} and estimate the optimal predictive model.

The best QSAR model was chosen based on the high Q^2, and the R^2 correlation coefficient should respect the following criterion ($Q^2 > 0.50$ and $R^2 > 0.60$) (25), while r^2_{ext} should have a value more than 0.6, which in turns indicates the significant predictability of the obtained QSAR model, and the combination of these positive results means that our model is reliable(EL-Mernissi et al., 2021).

2.4.Y-randomization

The Y-Randomisation was done to affirm the reliability of models obtained (Khalil EL Khatabi et al., 2020; Lafridi, Oussa, Zgou, & Bouachrine, 2020), where the independent variables of the studied molecules (pIC50) are shuffled several times randomly, and a new QSAR model is constructed after every iteration. It is possible to observe the randomized QSAR models with low Q^2 and R^2 values

compared to the original models due to structural redundancy and chance correlation, which indicate a reliable and robust 3D- QSAR model.

2.5 ADMET Prediction

Absorption of the chemical, distribution in the body, including biotransformation or metabolism, excretion, and toxicology are all part of pharmacokinetics (ADMET). This study used the SwissADME web server for predicting the ADMET properties (Daina, Michielin, & Zoete, 2017). ADMET prediction is an essential part of the discovery process, where the precise results help identify the best drug candidates.

2.6 Molecular Docking

To confirm the 3D- QSAR, we have analyzed the binding interactions between the TNIK protein (PDB code: 2X7F) and ligands. The surflex– Dock module of Sybyl was used for molecular docking studies. The pymol was used to carry out the docking protocol's stages (Delano, 2002). Consequently, the results were observed by using Discovery Studio 2016("Free Download: BIOVIA Discovery Studio Visualizer—Dassault Systèmes,").

2.7 Macromolecule and ligand preparations

The TNIK protein structure (PDB code: 2X7F) obtained from the Protein Databank PDB site (www.rcsb.org) was prepared using Discovery Studio 2016. Using the SKETCH option in Sybyl software, the 3D structure of compound 23 and the proposed compounds was formed. Three-dimensional structures were minimized under the Tripos standard force field with Gasteiger-Hückel atomic partial charges by conjugate gradient method with a gradient convergence criterion of 0.01 kcal/mol Å.

3. Results and Discussion

The best results were obtained by combining the two contours, such as, the CoMFA model has an excellent value of non-cross-validated (R^2 = 0.86), Standard error of the estimate (Scv = 0.19), F of 124.92, with a cross-validated Q^2 (0.65), and an optimum number of components of four. Subsequently, these models showed that the electrostatic field has the highest contribution in this model with a value of 46%, while the steric field is found to be 54%, and the external validation indicated the r_{ext}^2 value of 0.96. The CoMSIA model yielded excellent results in terms of R^2= 0.96, cross-validated Q^2=0.74, coefficient value of external validation r_{ext}^2 =0.95, an optimum component of 4, test value F=126.91, and standard error of the estimate Scv=0.18. The contributions of an electrostatic, steric, hydrophobic, H-bond donor and acceptor field were 23%, 20%, 22%, 17%, and 18%, respectively. The statistical results are displays in **table 2**, while **table 3** displays the experimental and predicted pIC50 values of the best models.

Table 2. The PLS statistical results of methods models.

Model	Q^2	R^2	S_{CV}	F	N	r_{ext}^2	FRACTION				
							Ster	Elec	Acc	Don	Hyd
CoMFA	0.65	0.86	0.19	124.92	4	0.96	0.54	0.46	-	-	-
CoMSIA	0.74	0.96	0.18	126.91	4	0.95	0.20	0.23	0.18	0.17	0.22

Table 3. The experimental and predicted pIC50 values of the models.

N	pIC_{50} (M)	Predicted		N	pIC_{50} (M)	Predicted	
		CoMFA	CoMSIA			CoMFA	CoMSIA
1*	7.85	8.04	8.02	**17**	8.42	8.55	8.61
2	7.85	7.09	7.08	**18**	8.10	8.24	8.11
3	7.72	7.63	7.59	**19**	9.64	9.41	9.51
4	9.04	9.14	9.02	**20**	9.68	9.50	9.57
5	7.82	7.96	7.81	**21**	9.60	9.71	9.88
6	7.37	7.44	7.46	**22**	9.74	9.62	9.63
7	7.57	7.37	7.26	**23**	9.92	10.01	9.98
8	7.92	8.06	8.12	**24**	9.68	9.72	9.74
9	8.15	8.24	8.34	**25**	9.66	9.92	9.52
10*	7.74	7.93	7.73	**26**	9.66	9.75	9.70
11*	9.89	9.72	9.93	**27**	9.33	9.40	9.38
12*	9.72	9.98	10.00	**28**	9.48	9.62	9.52
13*	9.37	9.69	9.56	**29***	9.10	9.36	9.38
14	8.28	8.14	8.32	**30**	9.52	9.40	9.60
15	7.51	7.47	7.41	**31**	9.17	9.25	9.21
16	9.36	9.45	9.71				

3.1 Graphical interpretation of CoMFA and CoMSIA

The CoMFA/CoMSIA contour maps were built to visualize the model field distribution where changes may result in an increase in activity. **Figures 3** and **Figure 4** display the CoMFA and CoMSIA contour maps, respectively. The compound 23 was employed as a reference structure, and all the contours represented the default 80% and 20% level contributions for favored and unfavored regions.

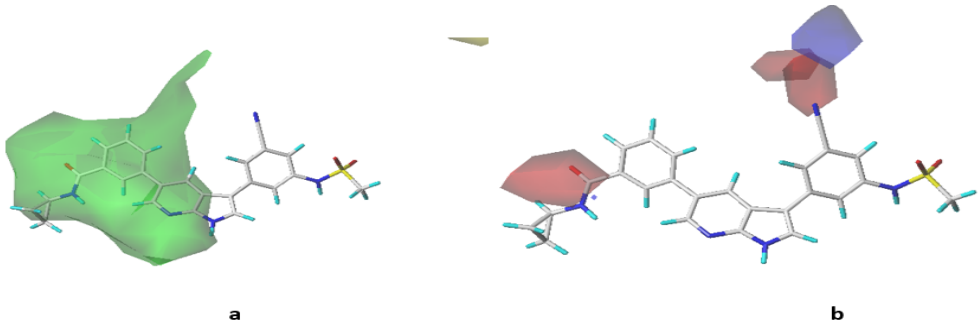

Figure 3. CoMFA field. a: Steric, b: electrostatic

The steric contour maps (Fig, 3a). The green color appeared around Ar1 substitution, indicating that bulky substitutions selection is necessary for this position (increase activity), this can explain the higher activity of compounds 23 (pIC50 = 9.92) having N-cyclopropylbenzamide in this position, compared to the compound 30 (pIC50 = 9.52) having N-methylbenzamide group at this position.

The electrostatic contour maps (Fig, 3b). The blue color is founded close to CN substitute, indicating that substituents with electron-donor character are favored at these positions (increased activity). A slight red contour near the N-methylformamide which belongs to group Ar1, indicating regions where more negative charges are favorable for the activity. This explains the higher activity of compound 23 (pIC50 = 9.92) has a bulky electron acceptor group compared to compound 22 (pIC50 =9.74) has a not bulky electron acceptor group.

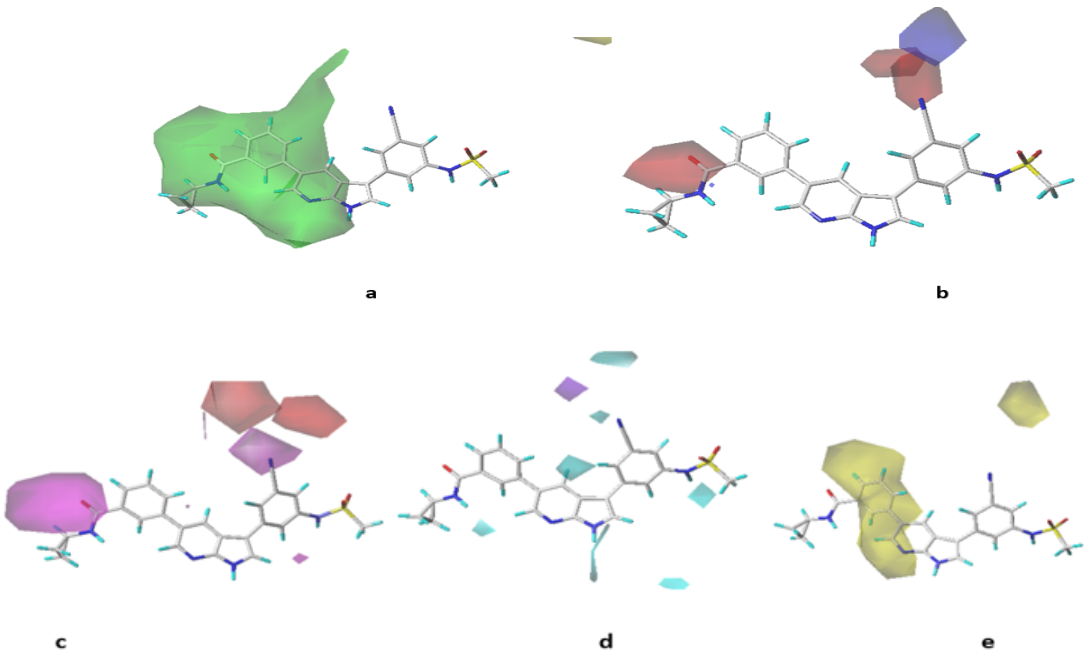

Figure 4. CoMSIA field. a: Steric, b: electrostatic, c: H-bond acceptor, d: Hydrogen-bond donor, e: Hydrophobic

The fields of CoMSIA are presented in Fig 4 (a, b, c, d, and e). According to figure (a) and (b), we haven't addressed the steric and electrostatic fields because are same in both contours, according to table 2, the other hydrophobic, hydrogen-bond donor and acceptor fields have a percentage 22%, 17% and 18% successively. The hydrogen bond acceptors contour maps (Fig, 4c). The colors red and magenta denote favorable and unfavorable locations for hydrogen donor groups to boost anticancer activity. The magenta contour around the N-methylformamide which belongs to Ar1 position and the CN group which belongs to the other side, indicates that an H-bond acceptor substituent at this position increases the activity, while the red appears not closer of CN group, this clarifies the higher activity of compounds 4 (pIC50 = 9.04) has a CN in this position, compared to the compound 1 (pIC50 = 7.85) have not any group at this position.

The hydrogen bond donor contour maps (Fig, 4d). The colors cyan and purple denote favorable and unfavorable locations for hydrogen donor groups to boost anticancer activity. The cyan emerged in the vicinity of the 1H-pyrrolo [2,3-b] pyridine and CN replacements, indicate that an H-bond donor substituent at this position increases the activity, while the purple appears not closer of CN group. The hydrophobic contour maps (Fig, 4e). The colors yellow and white indicate that hydrophobic groups enhance and reduce anticancer activity successively. The yellow color located all benzene, which belongs to Ar1 position, indicates that hydrophobic substituent at this position increases the activity.

3.2 Y – randomization

The pIC50 values were randomly mixed to test the models' durability, and a new QSAR model was generated after each rounding. The new values of Q^2 and R^2 are not acceptable because (Q^2 <0.5, R^2 <0.6), indicating that our optimal models are not due to a chance correlation. Q^2 and R^2 values of the generated models after several Y–randomization tests are shown in **Table 4**.

Table 4. Q^2 and R^2 values after several Y – randomization tests.

Iteration	CoMFA		CoMSIA	
	Q^2	R^2	Q^2	R^2
1	-0. 358	-0.426	-0.258	-0.442
2	0.285	0.394	0.176	-0.181
3	0.190	0.232	0.263	0.395
4	-0.330	-0.261	-0.284	-0.189
5	0.212	0.415	0.113	0.224

3.3 Newly designed compounds

We designed five compounds with greater biological activity than the most active chemical molecule in the database using 3D QSAR modeling. **Table 5** displays the pIC50 values and structures of these molecules.

Table 5. The structures of new molecules and their pIC50 values.

			Predicted pIC_{50}	
N°	**R_1**	**R_2**	**CoMFA**	**CoMSIA**
23	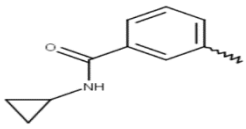	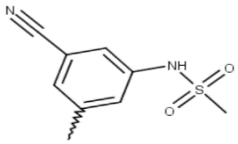	10.01	9.98
Y_1	-	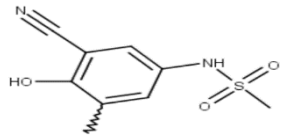	10.30	10.28
Y_2	-	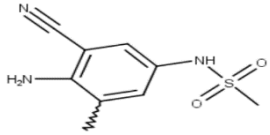	10.25	10.18
Y_3	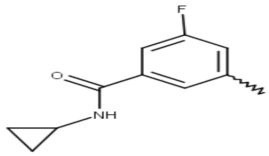	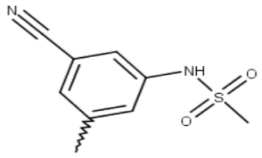	10.22	10.17
Y_4	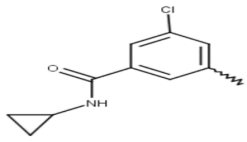	-	10.18	10.12
Y_5	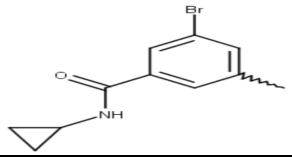	-	10.10	10.06

3.4 ADMET prediction

Absorption, distribution, metabolism, excretion, and toxicity (ADMET) characterization are crucial stages in predicting pharmacological properties. These characteristics were determined by utilizing Swissadme and the pKSM online tool in that order. **Table 6** shows the ADMET prediction of compound 23 and the proposed compounds (Y1-Y5).

Table 6. ADMET prediction of the most potent C_{23} and newly designed inhibitors.

Models		Compounds					
		C_{23}	Y_1	Y_2	Y_3	Y_4	Y_5
Absorption (A)							
Water solubility logS (log mol/L)		-3.58	-3.30	-3.28	-3.86	-3.65	-3.66
Intestinal absorption (human)		90.26	80.71	79.85	86.559	91.38	91.12
$Caco_2$ perm.(log Papp in10^{-6} cm/s)		0.71	0.41	0.58	0.58	0.81	0.92
Distribution (D)							
Blood-brain barrier (logBB)		-1.375	-1.55	-1.43	-1.56	-1.55	-1.57
Volume of distributionV_{DS}		0.16	0.12	0.22	0.15	0.58	0.46
Metabolism (M)							
Substrate (CYP)	2D6	No	No	No	No	No	No
	3A4	Yes	Yes	Yes	Yes	Yes	Yes
Inhibition (CYP)	1A2	Yes	Yes	Yes	Yes	Yes	Yes
	2C19	Yes	Yes	Yes	Yes	Yes	Yes
	2C9	Yes	Yes	Yes	Yes	Yes	Yes
	2D6	Yes	Yes	Yes	Yes	Yes	Yes
	3A4	Yes	Yes	Yes	Yes	Yes	Yes
Excretion (E)							
Clearence		0.43	0.32	0.45	0.34	0.97	0.72
Toxicity (T)							
AMES toxicity		No	No	No	No	No	No

Compound's absorption is controlled by intestinal absorption (human), water solubility, and Caco2 permeability. A drug's solubility in both water and lipids is a key element in its therapeutic action. Indeed, the medicine must go through numerous channels in the body to reach its target.

Every compound's solubility in water has a significant impact on its absorption and distribution, compounds with low solubility in water (logS) will have a poor absorption scheme. The predicted water solubility value of most medications on the industry is > -4, the poor absorbance the absorbance value is less than 30%, and the absorption of orally delivered medicines is predicted using Caco2 permeability, if the predictive value is more than 0,90, it is said to have a high Caco2 permeability. In the table above, all the suggested compounds have logS value > -4, a number higher than 75% of the level of intestinal absorption, and good permeability, these compounds are solubility in water, absorbed via the intestines of humans, and good permeable.

To assess the distribution factor, the Blood-Brain Barrier (logBB) and Volume of Distribution (VDS) were used. More medication reaches the brain when the volume of distribution is larger. Compounds with a logBB value < -1 will be poorly disseminated into the brain, but those with a logBB value > 0.3 will be cross BBB. All compounds have a logBB value < -1 that they will be poorly distributed into brain. The volume of distribution (VDS) is a parameter characterizing the distribution of the active substance in the human body. The values are accepted if values (VDss)> 0.45, the results obtained show that only the proposed Y4 and Y5 compounds have respected this value.

The results of metabolic parameters are more consistent, with some acceptable results. All the compounds (Y1-5) are inhibitors and substrates cytochrome, with the exception for 2D6 are not a substrate. The connection between drug concentration in the body and drug removal rate is described by the constant clearance, when the clearance value is greater, the medication is considered healthy to

take. The predicted compounds Y4 and Y5 have higher Clearance values and not toxicity, which indicates are the best drugs chosen.

3.5 Docking results

Molecular docking (Yang, B., et al. 2020; Diass. K., et al. 2023) is utilized to investigate and observe the 2D View binding modes of the C23 and proposed (Y1-5) compounds with the active site of Traf2 and Nck-interacting kinase (TNIK), the results given in **table 7**.

Table 7. 2D interactions of the ligands Y1-5 and C23 with TNIK receptor.

N°	2D View	N°	2D View
23	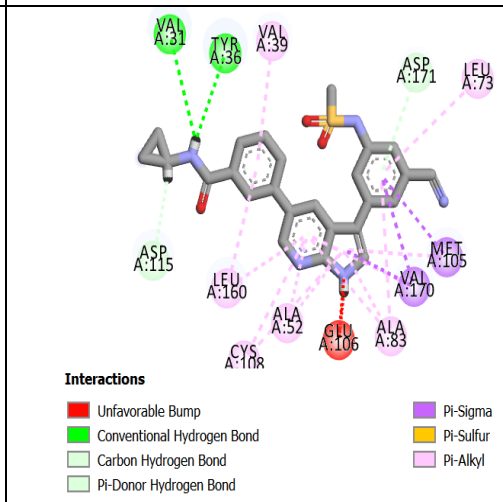	**Y_3**	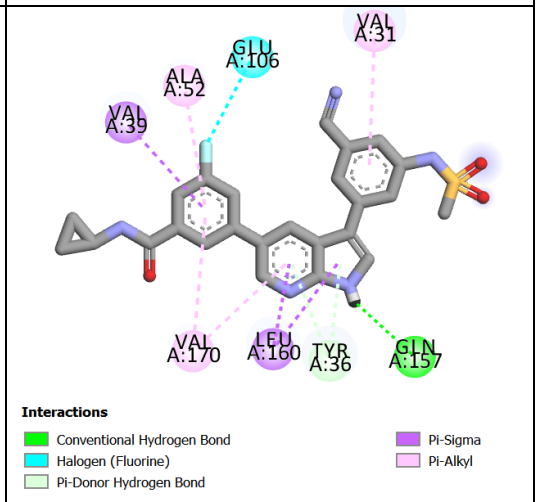
Y1	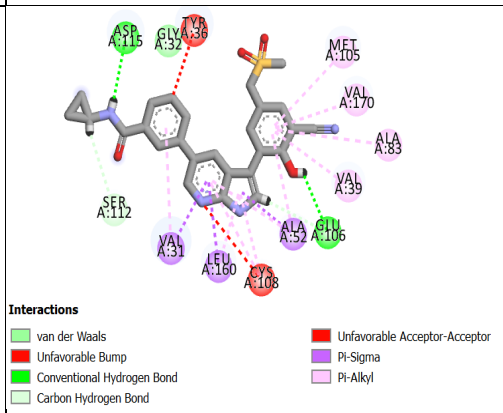	**Y4**	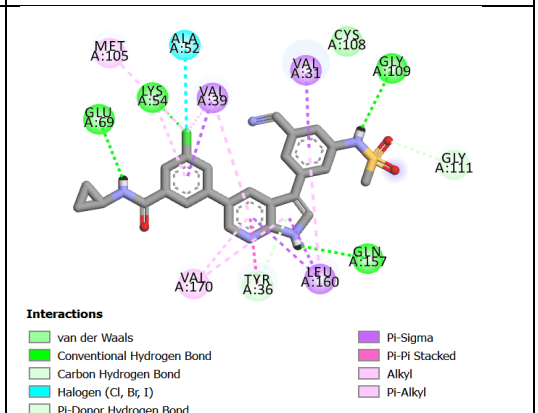
Y2	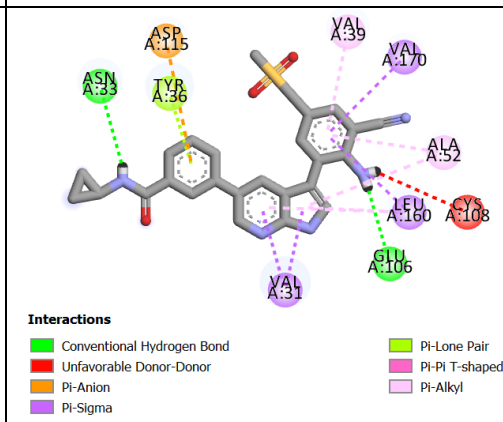	**Y5**	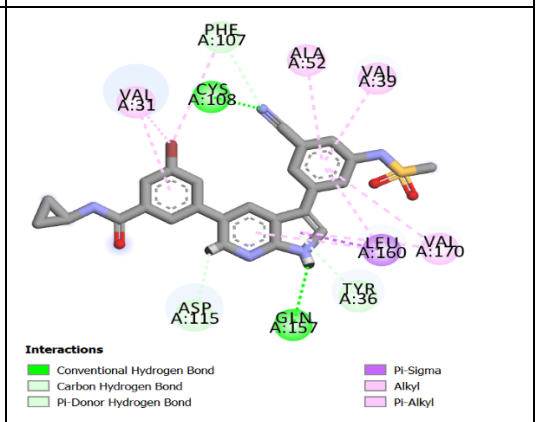

The stability of these complexes is increased by the presence of typical hydrogen bond interactions in all the component, while C23, Y1, and Y2 components have an unfavorable type of interaction. Furthermore, to continue comparing the stability of these compounds, table 8 shows the types of interactions and total scoring.

Table 8. Types of interaction and total scoring.

N°	Types of interactions		Total scoring
	Hydrogen Bond	Unfavorable Interaction	
C_{23}	VAL A:31, TYR A:36.	Glu A: 106	2.83
Y_1	ASP A: 115, GLU A:106, CYS A: 108.	TYR A: 36, CYS A:108.	2.63
Y_2	ASN A: 33, GLU A:106.	LYS A:108.	3.05
Y3	GLN A: 157 .		3.19
Y_4	GLU A: 69, LYS A:54, GLY A: 109, GLN A: 157.		3.64
Y_5	CYS A: 108, GLN A:157.		3.43

The predicted compounds have total score values between 2.05 and 3.64, which are higher than the reference ligand C23 (2.83), except for the Y1 component, which has a value of 2.63, because it has two unfavorable interactions.

The predicted component Y2 has two Hydrogen Bond interactions and one unfavorable interaction, while Y3 has just one Hydrogen Bond interaction type, this explains why these components are less stable compared to others.

The best ligands, Y4 and Y5, created four and three conventional hydrogen bonds, respectively, and not formed any unfavorable interactions. The reference ligand C23 has two conventional hydrogen bonds and one unfavorable interaction type, which explains why the predicted molecules Y4 and Y5 were more stable. Which we can conclude that the designed compounds (Y4 and Y5) are the most potent TNIK inhibitors against colorectal cancer cells.

Conclusion

In this research, a series of thirty-one 1H-pyrrolo [2,3-b] pyridine derivatives were investigated utilizing 3D-QSAR via CoMFA and CoMSIA models as effective TNIK inhibitors against colorectal cancer cells, demonstrating efficient predictability and stability. The contour maps produced by the 3D-QSAR model are the most important structural characteristics in terms of possible activity-increasing by favorable replacements. Consequently, based on the valuable guidelines developed by 3D-QSAR, five novels 1H-pyrrolo[2,3-b]pyridine derivatives were proposed with high activity against cancer. The ADMET was utilized to determine the pharmacokinetic characteristics and molecular docking was performed to validate them. The results show Y4 and Y5 were the most stable and active anti-cancer activities. It is important to synthesize these compounds to use them against colorectal cancer.

Disclosure statement: *Conflict of Interest:* The authors declare that there are no conflicts of interest.

Compliance with Ethical Standards: This article does not contain any studies involving human or animal subjects.

References

Bouamrane S., Khaldan A., Hajji H., El-mernissi R., Maghat, H., Ajana, M. A., Sbai, A., et al. (2022) 3D-QSAR, molecular docking, molecular dynamic simulation, and ADMET study of bioactive compounds against candida albicans. *Moroccan Journal of Chemistry,* 10(3), 10–541. Retrieved October 28, 2022, from https://revues.imist.ma/index.php/morjchem/article/view/33141.

Bujak A., Stefaniak, F., Zdzalik, D., Grygielewicz, P., Dymek, B., Zagozda, M., Gunerka, P., et al. (2015) Discovery of TRAF-2 and NCK-interacting kinase (TNIK) inhibitors by ligand-based virtual screening methods. *MedChemComm*, 6(8), 1564–1572. The Royal Society of Chemistry. Retrieved October 28, 2022, from https://pubs.rsc.org/en/content/articlelanding/2015/md/c5md00090d

Bush B. L., & Nachbar, R. B. (1993) Sample-distance partial least squares: PLS optimized for many variables, with application to CoMFA. *Journal of Computer-Aided Molecular Design*, 7(5), 587–619.

Clark M., Cramer, R. D., & Van Opdenbosch, N. (1989) Validation of the general purpose tripos 5.2 force field. *Journal of Computational Chemistry*, 10(8), 982–1012. http://doi.wiley.com/10.1002/jcc.540100804.

Cramer R. D., Patterson, D. E., & Bunce, J. D. (1988) Comparative molecular field analysis (CoMFA). 1. Effect of shape on binding of steroids to carrier proteins. *Journal of the American Chemical Society*, 110(18), 5959–5967. Retrieved August 12, 2022, https://pubs.acs.org/doi/abs/10.1021/ja00226a005.

Cronin K. A., Lake, A. J., Scott, S., Sherman, R. L., Noone, A.-M., Howlader, N., Henley, S. J., et al. (2018, July 1). Sybyl-X Molecular Modeling Software Package. S TRIPOS Associates. https://onlinelibrary.wiley.com/doi/10.1002/cncr.31551.

Daina A., Michielin, O., & Zoete, V. (2017) SwissADME: A free web tool to evaluate pharmacokinetics, drug-likeness and medicinal chemistry friendliness of small molecules. *Scientific Reports*, 7, 42717.

Delano W. (2002). The PyMOL Molecular Graphics System. *Undefined*. Retrieved June 15, 2022, from https://www.semanticscholar.org/paper/The-PyMOL-Molecular-Graphics-System-Delano/45b98fcf47aa90099d3c921f68c3404af98d7b56

Dow L. E., O'Rourke, K. P., Simon, J., Tschaharganeh, D. F., van Es, J. H., Clevers, H., & Lowe, S. W. (2015) Apc Restoration Promotes Cellular Differentiation and Reestablishes Crypt Homeostasis in Colorectal Cancer. *Cell*, 161(7), 1539–1552.

El Khatabi K., Aanouz, I., El-mernissi, R., Khaldan, A., Ajana, M. A., Bouachrine, M., & Lakhlifi, T. (2020) 3D-QSAR and Molecular Docking Studies of p-Aminobenzoic Acid Derivatives to Explore the Features Requirements of Alzheimer Inhibitors. *Orbital: The Electronic Journal of Chemistry*, 12(4), 172–181. August 18, 2021, http://orbital.ufms.br/index.php/Chemistry/article/view/1467.

El-Mernissi R., El khatabi, K., Khaldan, A., Bouamrane, S., ElMchichi, L., Aziz Ajana, M., Lakhlifi, T., et al. (2022) 3D-QSAR, ADMET and Docking Studies for Design New 5,5-Diphenylimidazolidine-2,4-dione Derivatives Agents Against Cervical Cancer. *Orbital: The Electronic Journal of Chemistry*, 14(1), 24–32. October 9, 2022, from http://orbital.ufms.br/index.php/Chemistry/article/view/1659

EL-Mernissi R., EL Khatabi, K., Khaldan, A., El Mchichi, L., Ajana, M. A., Lakhlifi, T., & Bouachrine, M. (2021) Design of new 3, 5-disubstituted indole as hematological anticancer agents using 3D-QSAR, molecular docking and drug-likeness studies. *Materials Today: Proceedings*, *The Fourth edition of the International Conference on Materials & Environmental Science,* 45, 7608–7614. https://www.sciencedirect.com/science/article/pii/S221478532102099X.

El-Mernissi R., El Khatabi, K., Khaldan, A., ElMchichi, L., Shahinozzaman, M., Ajana, M. A., Lakhlifi, T., et al. (2021) 2-Oxoquinoline Arylaminothiazole Derivatives in Identifying Novel Potential Anticancer Agents by Applying 3D-QSAR, Docking, and Molecular Dynamics Simulation Studies. *Journal of the Mexican Chemical Society*, 66(1). https://www.jmcs.org.mx/index.php/jmcs/article/view/1578.

EL-Mernissi R., Khatabi, K. E., Khaldan, A., Ajana, M. A., Bouachrine, M., & Lakhlifi, T. (2020) Discoveryof orthotolyloxyacetamides as inhibitors of NOTUM using 3D- QSAR and molecular docking studies. *Journal of Materials and Environmental Science*, 11(6), 952–962.

El-Mernissi R., Khatabi, K. E., Khaldan, A., Bouamrane, S., El, L., Ajana, M. A., Lakhlifi, T., et al. (2022) Designing of Novel Quinolines Derivatives as Hepatocellular Carcinoma Inhibitors by Using In silico Approaches. *Biointerface Research in Applied Chemistry*, 13(1), 15.

Free Download: BIOVIA Discovery Studio Visualizer—Dassault Systèmes. (n.d.). . Retrieved August 15, 2022, from https://discover.3ds.com/discovery-studio-visualizer-download

Jemal A., Bray, F., Center, M. M., Ferlay, J., Ward, E., & Forman, D. (2011) Global cancer statistics. *CA: A Cancer Journal for Clinicians*, 61(2), 69–90. http://doi.wiley.com/10.3322/caac.20107

Yudai Imai, Wakasugi D., Suzuki R., Kato S., Sugisaki M., Mima M., Miyagawa H., Endo M., Fujimoto N., Fukunaga T., Kato S., Kuroda S., Takahashi T., Kakinuma H., (2023) Lead identification of novel tetrahydroimidazo[1,2-a]pyridine-5-carboxylic acid derivative as a potent heparanase-1 inhibitor, *Bioorganic & Medicinal Chemistry Letters,* 79, 129050, https://doi.org/10.1016/j.bmcl.2022.129050

Kahn M. (2014). Can we safely target the WNT pathway? *Nature Reviews. Drug Discovery*, 13(7), 513–532.

Katanoda K., Ajiki, W., Matsuda, T., Nishino, Y., Shibata, A., Fujita, M., Tsukuma, H., Loka A., Soda M., Sobue T. (2012) Trend analysis of cancer incidence in Japan using data from selected population-based cancer registries. *Cancer Science*, 103(2), 360–368. https://onlinelibrary.wiley.com/doi/abs/10.1111/j.1349-7006.2011.02145.x

Khaldan A., Bouamrane, S., El-mernissi, R., Maghat, H., Ajana, A., Sbai, A., Bouachrine, M., et al. (2021) Identification of potential α-glucosidase inhibitors: 3D-QSAR modeling, molecular docking approach, *RHAZES: Green and Applied Chemistry*, 12, 60–75., fhttps://revues.imist.ma/index.php/RHAZES/article/view/26039

Khaldan A., Khatabi, K. E., El-mernissi, R., Sbai, A., Bouachrine, M., & Lakhlifi, T. (2020) Combined 3D-QSAR Modeling and Molecular Docking Study on metronidazole-triazole-styryl hybrids as antiamoebic activity. Moroccan Journal of Chemistry, 8(2), 8–539. https://revues.imist.ma/index.php/morjchem/article/view/19099.

Khatabi K El, El-Mernissi, R., Aanouz, I., Ajana, M. A., Lakhlifi, T., Shahinozzaman, M., & Bouachrine, M. (2022). Benzimidazole Derivatives in Identifying Novel Acetylcholinesterase Inhibitors: A Combination of 3D-QSAR, Docking and Molecular Dynamics Simulation. *Physical Chemistry Research*. 10(2), 13.

Khatabi Khalil EL, Aanouz, I., Ajana, A., Bouachrine, M., & Lakhlifi, T. (2021). In silico analysis of 3D QSAR and Molecular Docking studies to discover new thiadiazole-thiazolone derivatives as mitotic kinesin Eg5 inhibitors. *Moroccan Journal of Chemistry*, 9(3), 9–405. https://revues.imist.ma/index.php/morjchem/article/view/18721.

Khatabi Khalil EL, Aanouz, I., Khaldan, A., El-Mernissi, R., Ajana, M. A., Bouachrine, M., & Lakhlifi, T. (2020) PTP1B inhibitors for diabesity: Discovery of new bromophenol derivatives using 3D QSAR and Molecular Docking study, 9, 14. fhttps://revues.imist.ma/index.php/RHAZES/article/view/26039.

Klebe G., Abraham, U., & Mietzner, T. (1994) Molecular Similarity Indices in a Comparative Analysis (CoMSIA) of Drug Molecules to Correlate and Predict Their Biological Activity. *Journal of Medicinal Chemistry*, 37(24), 4130–4146. https://pubs.acs.org/doi/abs/10.1021/jm00050a010

Koutras A. K., Starakis, I., Kyriakopoulou, U., Katsaounis, P., Nikolakopoulos, A., & Kalofonos, H. P. (2011) Targeted therapy in colorectal cancer: Current status and future challenges. *Current Medicinal Chemistry*, 18(11), 1599–1612.

Lafridi H., Oussa, A., Zgou, H., & Bouachrine, M. (2020) QSAR modeling of antiradical properties of phenolic compounds using DFT calculations. *Moroccan Journal of Chemistry*, 8(4), 8–852. https://revues.imist.ma/index.php/morjchem/article/view/20579

de Lau W., Peng, W. C., Gros, P., & Clevers, H. (2014)The R-spondin/Lgr5/Rnf43 module: Regulator of Wnt signal strength. *Genes & Development*, 28(4), 305–316.

Li X., Wei W., Tao L., Zeng J., Zhu Y., Yang T., Wang Q., TangM., Liu Z., Yu L., (2023). Design, synthesis and biological evaluation of a new class of 7H-pyrrolo[2,3-d]pyrimidine derivatives as Mps1 inhibitors for the treatment of breast cancer, *European Journal of Medicinal Chemistry*, 245, Part 1, 114887, ISSN 0223-5234, https://doi.org/10.1016/j.ejmech.2022.114887.

Masuda M., Uno, Y., Ohbayashi, N., Ohata, H., Mimata, A., Kukimoto-Niino, M., Moriyama, H., et al. (2016) TNIK inhibition abrogates colorectal cancer stemness. *Nature Communications*, 7(1), 12586. Retrieved June 22, 2021, from http://www.nature.com/articles/ncomms12586

Morin P. J., Sparks, A. B., Korinek, V., Barker, N., Clevers, H., Vogelstein, B., & Kinzler, K. W. (1997) Activation of beta-catenin-Tcf signaling in colon cancer by mutations in beta-catenin or APC. *Science (New York, N.Y.)*, 275(5307), 1787–1790.

Okuno K. (2007) Surgical treatment for digestive cancer. Current issues—Colon cancer. *Digestive Surgery*, 24(2), 108–114.

Omura K. (2008) Advances in chemotherapy against advanced or metastatic colorectal cancer. *Digestion*, *77 Suppl 1*, 13–22.

Polakis P. (2000) Wnt signaling and cancer. *Genes & Development*, 14(15), 1837–1851. doi/10.1101/gad.14.15.1837.

Powell S. M., Zilz, N., Beazer-Barclay, Y., Bryan, T. M., Hamilton, S. R., Thibodeau, S. N., Vogelstein, B., et al. (1992) APC mutations occur early during colorectal tumorigenesis. *Nature*, 359(6392), 235–237. Nature Publishing Group. https://www.nature.com/articles/359235a0.

Purcell W. P., & Singer, J. A. (1967) A brief review and table of semiempirical parameters used in the Hueckel molecular orbital method. *Journal of Chemical & Engineering Data*, 12(2), 235–246. American Chemical Society. https://doi.org/10.1021/je60033a020.

Wielenga V. J., Smits, R., Korinek, V., Smit, L., Kielman, M., Fodde, R., Clevers, H., et al. (1999) Expression of CD44 in Apc and Tcf mutant mice implies regulation by the WNT pathway. *The American Journal of Pathology*, 154(2), 515–523.

Yamamoto Y., Sakamoto, M., Fujii, G., Tsuiji, H., Kenetaka, K., Asaka, M., & Hirohashi, S. (2003) Overexpression of orphan G-protein–coupled receptor, Gpr49, in human hepatocellular carcinomas with β-catenin mutations. *Hepatology*, 37(3), 528–533. https://doi.org/10.1053/jhep.2003.50029

Yang B., Wu, Q., Huan, X., Wang, Y., Sun, Y., Yang, Y., Liu, T., et al. (2021) Discovery of a series of 1H-pyrrolo[2,3-b]pyridine compounds as potent TNIK inhibitors. *Bioorganic & Medicinal Chemistry Letters*, 33, 127749. https://linkinghub.elsevier.com/retrieve/pii/S0960894X2030860X.

Diass K., Oualdi I., Dalli M., Azizi S.-Ed, Mohamed M., Gseyra N., Touzani R., Hammouti B. (2023) Artemisia herba alba Essential Oil: GC/MS analysis, antioxidant activities with molecular docking on S protein of SARS-CoV-2, *Indonesian Journal of Science & Technology* 8(1) 1-18.

(2023) ; https://revues.imist.ma/index.php/morjchem/index